Auton Robot (2010) 28: 457–470
DOI 10.1007/s10514-010-9179-y

Ground adaptive and optimized locomotion of snake robot moving with a novel gait

Shahir Hasanzadeh · Ali Akbarzadeh Tootoonchi

Received: 8 September 2008 / Accepted: 4 March 2010 / Published online: 24 March 2010

Abstract In this paper, we present a novel gait, forward head serpentine (FHS), for a two dimensional snake robot. The advantage of this new gait is that the head link remains in the forward direction during motion. This feature significantly improves snake robot potential applications. Genetic Algorithm (GA) is used to find FHS gait parameters. Relationship between FHS gait parameters and friction coefficients of the ground are developed. Next, robot speed is considered in the optimization. A fitness function covering robot speed and head link angular changes is defined. A general sinusoidal wave form is applied for each joint. GA is used to find gait parameters resulting in maximum speed while head link angular changes remain in an acceptable range. Optimal gait parameters are also calculated for different friction coefficients and relationships between them are developed. Experiments are also performed using a 5-link snake robot. It is shown that experimental and theoretical results closely agree.

Keywords Snake robot · Novel gait · Locomotion · Serpentine · Genetic algorithm

1 Introduction

Snake robots are serially connected, multilink articulated mechanisms, which propel themselves by body shape undulations. Despite having challenges in the area of control and inefficiency in locomotion due to high friction, snake robots have attracted the attention of researchers for applications not suitable for wheeled and legged robots. Applications such as ruins of collapsed buildings or narrow passages in search and rescue operations are good examples where snake robots may be used.

Snake robots offer advantages over wheeled vehicles due to their terrainability, high adaptability to environment (by using suitable locomotion modes also called gait) and increasing reliability due to their modular nature. However, the two main challenges of snake robots over wheeled mechanisms are difficulty in control of snake-like locomotion as well as their poor power efficiency. In the present paper, we contribute to the first disadvantage by introducing a novel gait. We also optimize the proposed gait in terms of speed. Additionally, we improve its terrainability, ability to avoid obstacles in an environment full of obstacles, by using optimized parameters for a given environmental condition.

Locomotion control of snake robot has been addressed by many researchers. Two broad classes of control methods have been used. The first class can be described as trajectory-tracking control. It uses predefined gait patterns, usually computed as sine waves that are tracked with a feedback controller (Hirose 1993). Typically, the control is open-loop with respect to receiving feedback from the environment. The joint positions are calculated and sent to the motor controllers, usually PID controllers.

The other class of controllers can be described as online gait generation control. In these cases, gaits are not predefined, but are generated online during locomotion. Approaches used for this class better deal with irregular terrains and are mostly model-based. They rely on a kinematic (Prautsch and Mita 1999 and Date et al. 2001) or dynamic (Ute and Ono 2002; Burdick et al. 1995; Chirikjian and Burdick 1995) model of the robot's locomotion in order to design control laws for the gait generation. The limitation of

S. Hasanzadeh · A.A. Tootoonchi (✉)
Department of Mechanical Engineering, Ferdowsi University of Mashhad, Mashhad, Iran
e-mail: ali_akbarzadeh_t@yahoo.com

this approach is that the performance of controllers will deteriorate when models become inaccurate.

One of the first known biologically inspired snake robot was built by Hirose and co-workers (Umetani and Hirose 1976). He generically named this kind of robot an active cord mechanism (ACM). He derived a curve to describe the gliding form of the snake that is mathematically expressed using Bessel functions. He called this function the serpenoid curve. He realized the serpentine undulation form of snake locomotion on physical model of robot by applying sinusoidal trajectories to the differential angles between adjacent links. Hirose has constructed several snake-like robots since that time including descendants of the ACM as well as the Koryu snake robots (Hirose and Morishima 1990; Endo et al. 1999; Fukushima et al. 1998). Each of these robots utilizes a serial-link structure and uses wheels to create a no side-slip condition for each link. Since that time, a plethora of research efforts from the robotics and general engineering communities have been concentrated on constructing snake robot models as well as realizing snake like locomotion (Chirikjian and Burdick 1993; Klaassen and Paap 1999; Choi and Ryew 2002; Saito et al. 2002).

Dowling (1997) used a table look-up method to determine locomotive patterns. He made the suggestion of using Fourier series coefficients as parameters for the functional form of the structure's body. He offered suggestion on selection of those parameters through learning methods. He also suggested the use of specific resistance as a measure of gait success. By applying his methods multiple gaits are demonstrated including non-snake-like gaits.

Date et al. (2000) introduced a control methodology for serial-link structure with a no side-slip condition based on the concept of dynamic manipulability. The proposed control technique attempts to compromise between motion in a desired direction while maintaining a suitably high measure of manipulability. The team also added the condition of minimizing the side constraint forces. They were able to achieve a smoothing or regularization effect and obtained a wave-like geometry which produced a locomotion that is strikingly similar to that obtained via sinusoidal differential angles.

Saito et al. (2002) constructed a snake-like serial link structure and designed PID and H_∞ controllers to control the orientation and speed of robot, respectively. While most of the existing powered-joints snake robots utilize passive wheels to realize serpentine locomotion, his work addressed prototype which crawled on their underside and did not rely on wheels.

McIsaac and Ostrowski (2000) studied snake robot locomotion theory based on Geometric Mechanics. Prautsch et al. (2000) reduced and simplified dynamic modeling of snake robots. Position control of the head of a snake robot has been studied by Matsuno and Sato (2005) based on dynamic model, and trajectory tracking is realized by considering the body of robot as a redundant manipulator. Tanev et al. (2005) studied automatic design of the fastest locomotion gait of a simulated snake robot (Snakebot) through genetic programming. Empirically obtained results demonstrated the emergence of sidewinding gait from relatively simple motion patterns of morphological segments. Recently, the control methodology based on central pattern generator is attracting attention as a methodology to realize adaptive online gait generation of robots having large degrees of freedom (Ijspeert 2001; Crespi et al. 2005). A central pattern generator is a neural circuit capable of producing coordinated patterns of rhythmic activity in open loop, i.e. without any rhythmic inputs from sensory feedback or from higher control centers.

2 Snake robot model

In this paper we consider a planar n-link snake robot with dynamically identical links. The robot model is composed of serially connected links. Between every two links, a one-dimensional joint rotating on vertical (yaw) axis is located. Similar to real life snakes, friction force between the robot body and the environment is large in normal direction and small in tangential direction. This is usually realized using passive wheels in snake robots. We derived dynamic equation of the robot using Lagrange's methods (submitted to Journal of Robotics and Autonomous Systems). The derived dynamic equation is used for all simulations throughout this paper. The dynamic equation can be summarized as

$$BT = M(\theta)\ddot{q} + H(\theta, \dot{\theta}) + F(\theta) \tag{1}$$

where $M(\theta)$ is the $(n+2) \times (n+2)$ positive definite and symmetric inertia matrix, $H(\theta, \dot{\theta})$ is the $(n+2) \times 1$ matrix related to centrifugal and Coriolis terms, $F(\theta)$ is an $(n+2) \times 1$ matrix related to friction forces, B is an $(n+2) \times (n-1)$ constant coefficient matrix. T is $(n-1) \times 1$ matrix of input torques and $\theta, \dot{\theta}, \ddot{\theta}$ are $n \times 1$ matrix of links absolute angles and their derivatives. Finally $q, \dot{q}, \ddot{q}$ are $(n+2) \times 1$ matrix of generalized coordinates and their derivatives. Generalized coordinate are defines as

$$q = [\theta_1, \theta_1, \ldots, \theta_n, x_b, y_b] \tag{2}$$

where (x_b, y_b) is coordinate of the end of tail link (Fig. 1). We consider a simple coulomb friction model for the interaction of snake robot with the ground as

$$f_{ei} = -m_i g \mu_e \operatorname{sign}(v_i^e) \tag{3}$$

where $e = t, n$ (t and n represents tangential and normal directions). g is the gravity constant. μ_t and μ_n are normal and tangential coulomb friction coefficients. Subscript

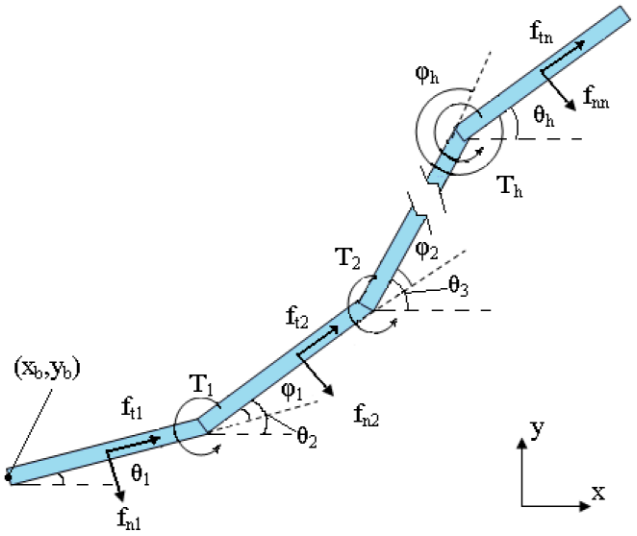

Fig. 1 Snake robot model

i corresponds to the ith link, f_{ti} and f_{ni} are friction forces in tangential and normal directions, respectively. v_i^t and v_i^n are velocities of the center of mass of i-th link. The signum function is denoted by sign(x); i.e., sign(x) is 1 if $x > 0$, 0 if $x = 0$, and -1 if $x < 0$.

3 Introduction of a novel gait

An important feature of snake robot is its capability to move with different gaits. Some of these gaits are biomimetic such as serpentine and rectilinear. Non biomimetic gaits are not used by real snakes but may be used by snake robots. For example parking gait introduced by McIsaac and Ostrowski (2000) which its motion resembles that of a car performing parallel parking maneuver. Brief introduction of snake gaits is available in literature (Dowling 1997).

In this section, we first review serpentine gait because it is the most commonly used mode of locomotion and its similarity to our proposed FHS gait. Next we will compare advantages and disadvantages of serpentine and FHS gaits.

3.1 Serpentine gait

The most straightforward way to generate traveling wave in a serial chain of n link is by having the joint angles vary sinusoidally with a common frequency and a constant phase lag between consecutive joints. The undulatory motion of a snake can be imitated by changing the relative angles of ith joint in the following manner (Saito et al. 2002):

$$\varphi_i = \alpha \sin(\omega t + (1-i)\beta) + \gamma \quad (i = 1, \ldots, n-1) \tag{4}$$

where α is the maximum angular deflection for each joint. β is the phase shift of any two adjacent relative angles. ω is frequency of locomotion which specifies how fast the serpentine wave propagates along the body and thus determines speed of locomotion. γ is the angular offset that provides a means for steering the mechanism and is set to zero for locomotion in straight line. If γ is non-zero the mechanism moves along a curved path, clockwise or counter clockwise, depending on the sign of offset γ. The wave propagation direction depends on the sign of β and is from link n to link 1 for positive β; if this wave propagation direction results in forward motion, then reversing this sign results in backward motion.

3.2 Novel gait—forward head serpentine (FHS)

In general, when snake is moving, it is preferable that its head remains in a fixed orientation directed towards the target. This can facilitate the processing of the information received from sensors such as vision system that are usually attached to the head link. We believe this added capability, is a step towards building an autonomous robot.

When snake robot moves with serpentine gait, its head link oscillates and therefore sensory information coming from a sensor attached to this link is constantly changing during motion. This makes the control more difficult especially in more autonomous snake robots equipped with multiple sensors or cameras.

In order to solve this problem we propose a novel gait that minimizes the orientation changes of the head link while the remaining links continue to follow a serpentine motion. We call this gait, forward head serpentine (FHS) gait because head link moves in forward direction while all other links move similar to serpentine gait (compare Fig. 2 and Fig. 5).

Relative angle of all links except the head link for driving an n-link robot to forward direction with FHS gait are

$$\varphi_i = \alpha \sin(\omega t + (1-i)\beta) + \gamma \quad (i = 1, \ldots, n-2) \tag{5}$$

The relative angle for the head link, $\phi_{h=}\phi_{n-1}$, is

$$\varphi_h = \alpha_h \sin(\omega t + \beta_h) + \gamma_h \tag{6}$$

where γ_h is steering parameter, α_h and β_h are maximum angular deflection and phase shift of the head link actuator, respectively. Parameters α_h and β_h have to be found for a given α and β to insure

- Minimum orientation changes for the head link as well as,
- Maintaining direction of head link along the direction of robot motion.

Comparing (4) with (5) and (6) one can find out that locomotion using FHS gait is decoupled into two separate tasks each generated by a separate parts of the snake robot body. First task uses head link to set the direction of motion by means of steering parameter γ_h used in (6). Second

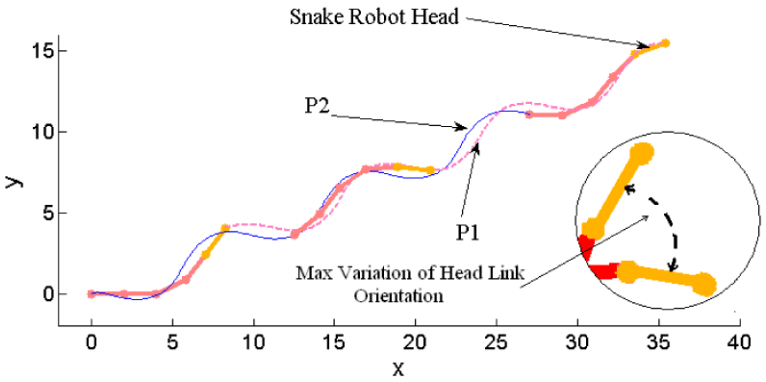

Fig. 2 Serpentine gait of snake robot: P1 is path followed by head, P2 is path followed by tail

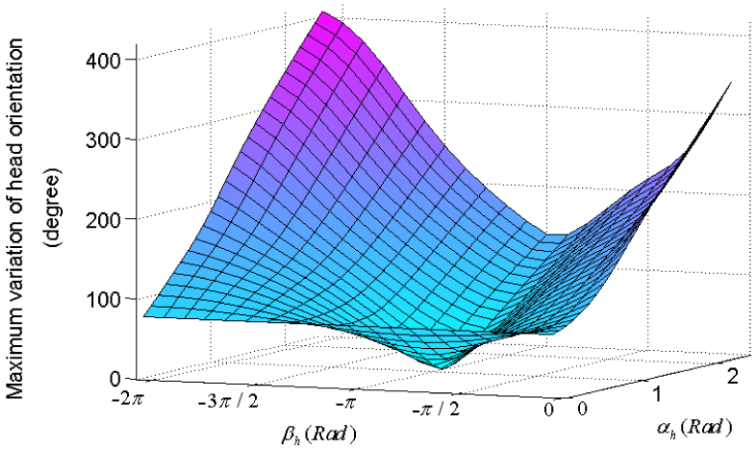

Fig. 3 Maximum variation of head link angle for different values of α_h and β_h ($\alpha = \pi/4$ and $\beta = \pi/4$)

task uses the remaining links to generate a traveling wave, (5), through the body of snake in order to propel the robot to the forward direction. As an analogy, consider a number of wagons that follow turns of the head wagon. Setting a nonzero value for γ_h results in turning motion of the robot in a circular path. Interestingly oscillation of the head remains low, even though robot turns. This feature will be better explained in Sect. 5.2.

4 Finding FHS gait parameters

The values of α and β of all actuators (joints) except the head link actuator can be selected arbitrarily. The value of β can be selected in the range of $[0, -2\pi]$ and value of α is limited to maximum allowable rotation angle of the joints. Therefore, one can select arbitrary values of $\alpha = \pi/4$ and $\beta = \pi/4$ for (5) and measure maximum variation of head link orientation during specific amount of time for different values of α_h and β_h. This will produces a smooth surface as shown in Fig. 3. The maximum variation of head link orientation is shown in Fig. 2 and is the difference between maximum and minimum angles that the head link makes with the horizontal line during its motion. Clearly for any other values of α and β similar surface can be obtained. Finding FHS gait parameters is equivalent to obtaining global minimum of this surface. As there is no local minimum in the surface, finding its global minimum is not a complicated task.

Problem of finding parameters of FHS gait is an optimization problem that can be solved with different methods. Since derivative of the objective function is not available only derivative-free optimization methods such as Simplex Search or Genetic Algorithm can be used. Although GA is computationally expensive, in this paper, we use it as optimization method since finding FHS gait parameters is an offline procedure. Additionally, we used GA for all optimization problems as we wanted to use one method for the entire paper. GA has widely been used in literature for optimization of complicated dynamic systems. GA imitates biological evolution. The target of optimization (FHS gait parameters α_h and β_h) are coded as chromosome and called genotype. Phenotype is the result of decoding of genotype (resultant robot locomotion, in this study) and is evaluated by the use of computer simulations. Genotypes with lower evaluation in gene pool will be deleted from the pool and remaining superior genotypes will succeed to next generation after being processed by genetic operators, i.e. mutation and crossover. By repeating this process, finally chromosomes with high quality can be derived. GA process steps are listed as follows:

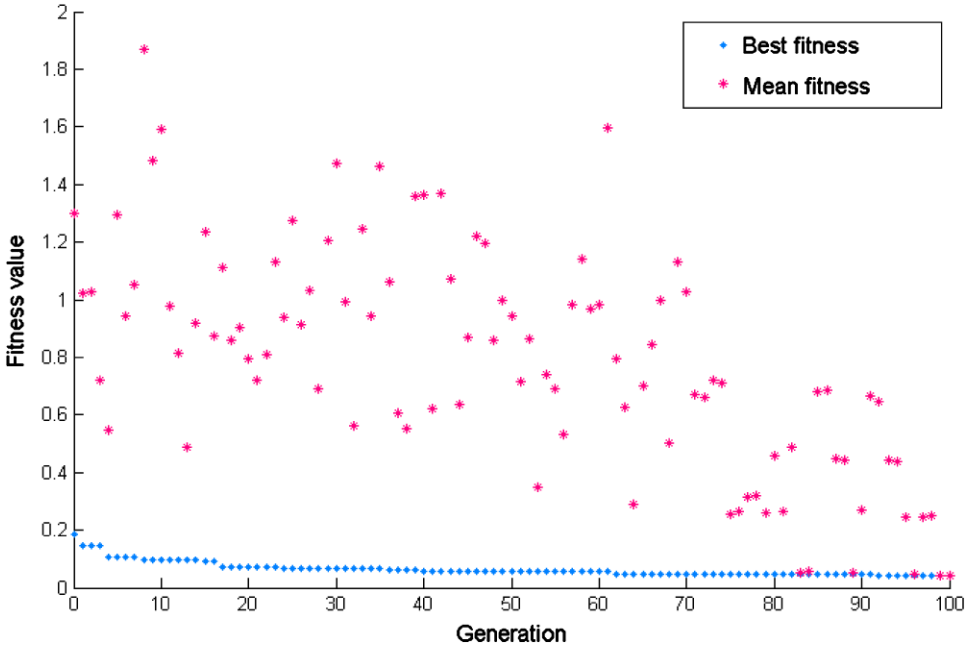

Fig. 4 Development of the best and mean value of fitness for every generation ($\alpha = \pi/6$, $\beta = \pi/3$ and $\omega = 1$)

- Coding—As genotype, we code chromosomes by serially connecting parameters discretized into 16-bit integers within given ranges. The resultant length of chromosomes become 32-bit (α_h and β_h). At the first stage of GA, new chromosomes are created by randomly setting parameters within ranges given to each parameter.
- Constraints—Because of mechanical limit of motor rotation angle, the value for the relative joint angle is also bounded as $\alpha_h + \gamma_h \leq \theta_{\max}$, where $\theta_{\max}$ is the maximum rotation angle of the head actuator. In this stage we assume γ_h is equal to zero which means robot moves in a straight line. Chromosomes not satisfying these values will be deleted and new random chromosome will be created.
- Fitness function—Fitness function in our study is a function of FHS parameters and is calculated by measuring orientation of the head link during the fixed time of locomotion simulation. The difference between minimum and maximum values of the measured head orientation is defined as fitness value that has to be minimized. Calculation of fitness function is related to mechanical dynamics of the robot as well as friction coefficients of the surface which the snake robot moves on. Therefore, during the simulation time, for a given (α, β) and environmental conditions (μ_t and μ_n) dynamic equation, (1) is solved and motion parameters $(q, \dot{q}, \ddot{q})$ are determined.
- Selection—Chromosomes are selected using roulette rule based on fitness value. We apply elite preservation method for fast convergence.
- Genetic operations—Between remaining chromosomes, crossover and mutation operation is applied. The way of cross over is one-point crossover with probability of P_c and mutation is performed by randomly reversing bits with a given probability P_m.

5 Results of GA

Based on the above-mentioned settings, GA finds FHS gait parameters. GA Conditions are as follow: Population $N = 10$, Crossover probability $P_c = 0.5$, Mutation probability $P_m = .01$, Number of generations $G = 100$ and $\theta_{\max} = \pi$.

We arbitrarily choose a set of serpentine gait parameters $\alpha = \pi/6$ rad, $\beta = \pi/3$ rad and $\omega = 1$ rad/s and show the development of fitness value (Fig. 4). In this example, the serpentine gait parameters remain constant and are the same for all actuators except head link actuator. Next, we use GA to find FHS parameters for the head link. Friction coefficients are assume to be $\mu_t = 0.05$ and $\mu_n = 0.56$. In Fig. 4. "best" and "mean" are the best fitness and mean value of the population, respectively. As shown in this figure, after 100 generations best fitness value converges to 0.035 that corresponds to $\alpha_h = 0.471$ rad, $\beta_h = -1.704$ rad. Using these FHS parameters, maximum value of orientation change for the head link is only 2.01 degrees.

5.1 Comparing FHS with serpentine gait

Two main characteristics of snake robot locomotion are speed of motion and input power. These characteristics are compared for serpentine and FHS gaits. To find FHS gait parameters, we must first choose a serpentine gait. Serpentine gait is selected by choosing a desired (α, β). FHS gait

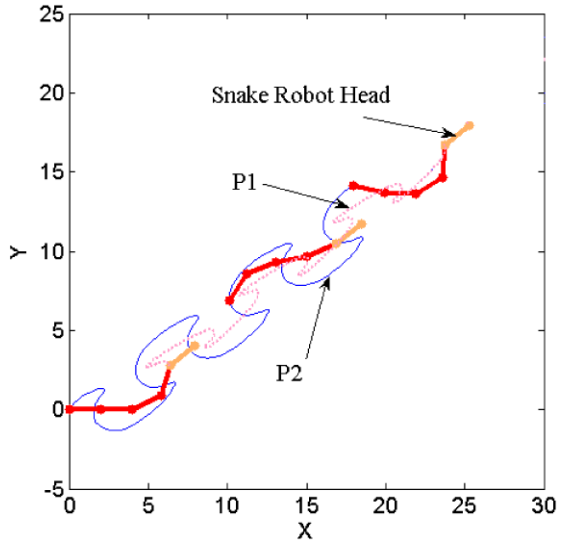

Fig. 5 Forward head serpentine gait of snake robot. P1 is path followed by head, P2 is path followed by tail

will use the given (α, β) for all actuators except the head actuators and find the optimum (α_h, β_h) for the head actuator. Next, a simulation is performed where both gaits are simulated in a same amount of time. Robot speed and input power for both gaits are calculated. Environment conditions (μ_t and μ_n) are also the same for both simulations.

Average velocity is calculated by determining displacement of center of mass of snake robot during the simulation time. Input power of any actuator, at any time, can be obtained by multiplying instantaneous input torque by angular velocity of the actuator. We use sum of the average values of the obtained signals as a measure of average input power for the robot.

We randomly choose three separate serpentine case studies. Results of the three sets of simulations are listed in Table 1 and Table 2. Table 1 shows the FHS parameters calculated by GA and Table 2 compares input power and speed of snake robot moving with serpentine and FHS gait (geometrical parameters for each link are: mass: 1 Kg, length: 1 m, moment of inertia: 0.33 Kg m^2).

As shown in Table 2, in case 1 and 2 velocity of serpentine gait is slightly higher than FHS gait and input power of serpentine gait is less than of FHS gait. Therefore, serpentine gait is likely to be more efficient than FHS. However, this is reversed in case 3 which shows faster speed and lower input power for the FHS gait.

From these results, we cannot derive a general statement regarding velocity and power efficiency advantages of one gait over another. Therefore, choosing the proper gait mostly dependents on the robot application.

Table 1 Finding FHS gait parameters

No.	α (rad)	β (rad)	α_h (rad)	β_h (rad)
1	$\pi/2$	$2\pi/5$	1.132	−1.268
2	$\pi/4$	$\pi/4$	0.768	−1.98
3	$3\pi/8$	$\pi/8$	1.528	−2.728

Table 2 Comparing serpentine with fhs gait

No.	Gait	Power (W)	Speed (cm/s)
1	FHS	84.92	60.61
	Serpentine	72.83	68.80
2	FHS	54.87	115.42
	Serpentine	42.50	160.68
3	FHS	216.16	119.16
	Serpentine	239.20	94.68

5.2 Turning

Another question is whether or not we can achieve FHS gait while turning. To answer this we run simulation for different values of γ which results in rotation of the robot with different turning radiuses. We used fixed values for α, β and environmental conditions (μ_t, μ_n) and found values of α_h and β_h versus head link orientation. See Fig. 6. By inspection of the obtained surfaces, without running an optimization, we can see that they are very similar and thus we may claim that γ does not significantly affect α_h and β_h. Therefore, we can conclude while snake robot turns, orientation of its head link remains minimum and head link remains in direction of motion (Fig. 7). As shown in Fig. 7, other links of the robot follow circular path of the head.

6 Considering adaptation to friction

In real world application of snake robot, environment conditions are not constant therefore snake robot should be adaptive to different environments. Or at least if it is designed for a specific environment, it should be less sensitive to environmental conditions. In our case, as was mentioned before we calculate FHS parameters for a specific friction coefficients. Therefore, we should investigate effectiveness of the designed FHS gait in environments with different friction coefficients. To do this, we need to find FHS gait parameters for different friction coefficients while other parameters remain constant (geometrical parameters are equal to our experimental snake robot and $\alpha = \pi/4$ rad, $\beta = \pi/4$ rad). Therefore, we run GA for each pair of normal and tangential friction coefficients (μ_t and μ_n) and find optimum FHS parameters (α_h, β_h). The selected range for friction coefficients is chosen to represent two extreme surfaces, wood and

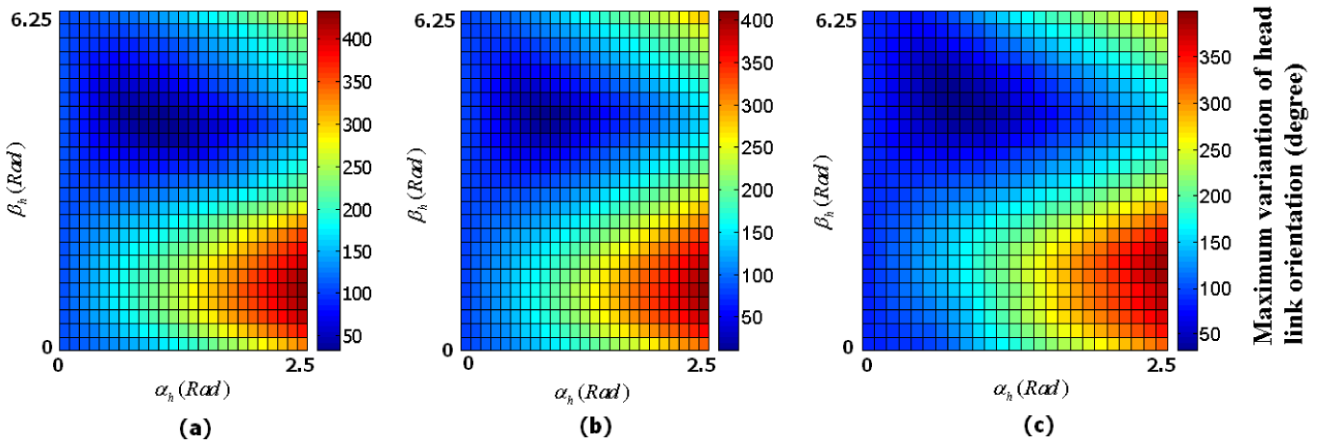

Fig. 6 Maximum variation of head link orientation for (**a**) $\gamma = -\pi/20$, (**b**) $\gamma = 0$, (**c**) $\gamma = \pi/20$

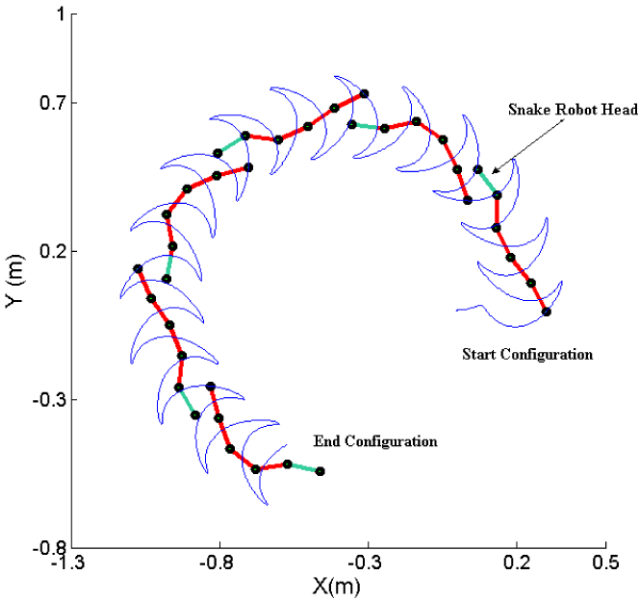

Fig. 7 Robot turning with forward head serpentine gait

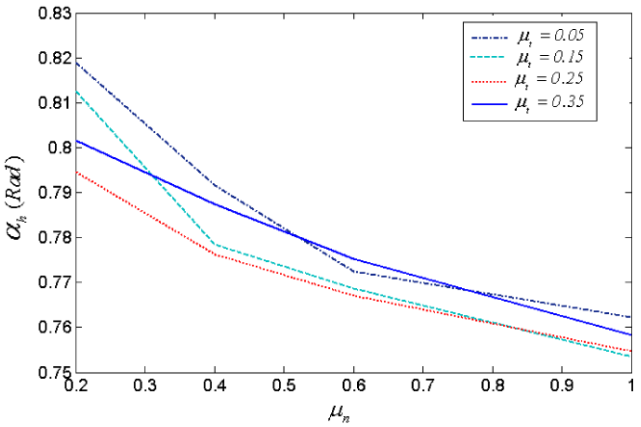

Fig. 8 Effect of different friction coefficients on α_h ($\alpha = \pi/4$ and $\beta = \pi/4$)

glass. Results are shown in Fig. 8 and Fig. 9. As illustrated in Fig. 8, μ_t does not have a considerable effect on α_h. But in the case of μ_n we can write

$$\alpha_h = -0.059\mu_n + 0.81 \tag{7}$$

This function can be used in a controller to alter FHS parameters while robot moves on different surfaces. Normal friction coefficient can be measured by means of force sensors mounted on the wheels (Inoue et al. 2007). As illustrated in Fig. 9, variations of μ_t effects β_h by less than 7% and that of μ_n effects β_h by less than 5%. Therefore, we believe that μ_t and μ_n do not have a considerable effect on β_h and remain mostly constant.

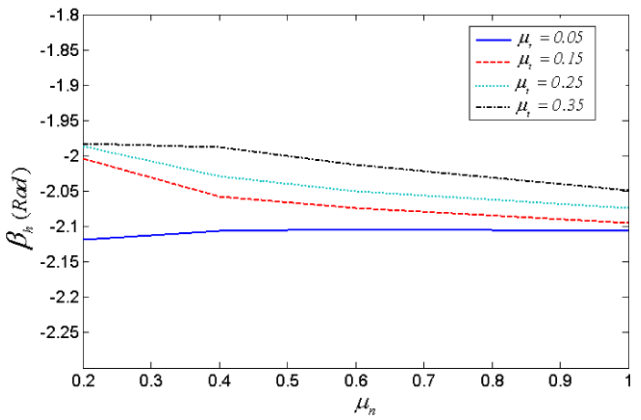

Fig. 9 Effect of different friction coefficients on β_h ($\alpha = \pi/4$ and $\beta = \pi/4$)

7 Optimization of FHS gait

In snake robots, it is friction force between each link and ground that generates forward motion. Therefore, they have less motion efficiency compare to other mobile robots. Considering the inherent power inefficiency of snake robots, it is important to study the conditions of efficient motions while robot moves with FHS gait. Optimally efficient motion of snake robot moving with serpentine gait has been studied by several authors (Saito et al. 2002; Ma et al. 2002). In this section our aim is to find FHS gait parameters that result in a motion with maximum speed. We consider two cases: the simpler one (Sect. 7.1) is to find α, β, α_h and β_h which maximize speed and minimize head orientation. We also consider more general form of the problem in Sect. 7.2.

7.1 Case I

In this case, GA is used to search for optimal FHS gait parameters $(\alpha, \beta, \alpha_h, \beta_h)$. The resultant length of chromosomes becomes 64-bit. Values of α and α_h are bounded to maximum value $(\theta_{\max})$ because of mechanical limit of motor rotation angle. Fitness function that is to be minimized is defined as

$$\text{Fitness Function} = \gamma \times \text{Orientation change of head link} + \frac{1}{\text{Speed}} \tag{8}$$

Obtaining fitness value of (8) calls for solving dynamic equation of the robot, (1). This will result in obtaining motion parameters $(q, \dot{q}, \ddot{q})$ of robot for the selected simulation time. Speed of the robot can be calculated by measuring distance traveled by robot during specified simulation time.

By defining fitness function as in (8), GA objective is divided into two parts with different priorities. The higher priority objective is to find motion with minimum orientation of the head link. Objective with lower priority is to maximize speed of motion. Parameter λ weights priority of the first task with respect to the second. Smaller values of λ result in robot motion with higher speed. Larger values of λ result in lower robot speed while maintaining the head link in the forward direction. We do not impose a hard constraint on value of maximum variation of the head link because our aim is to gain an insight into the relationship between speed and maximum variation of the head.

We run different optimizations with different values of λ. Figure 10 compares speed and orientation of head link for different λ. Through observing this figure we manually selected λ equal to 0.25 which maintains the variation of head link in an acceptable range of 8.6 degrees while center of mass of robot moves with speed of 4.7 cm/sec. Each application has a different acceptable range for the value of head link variation. We believe less than 10 degrees overall variation is acceptable for an application where a robot is equipped with a camera and the camera is viewed by an operator. The selected value for λ is rather arbitrary. Depending on the requirement of the task, the user may select $\lambda = 0.1$ which will result in speed increase but will also increase the variation of the head link. Alternatively, if situations calls for minimum head link variation, the user may select $\lambda = 0.75$.

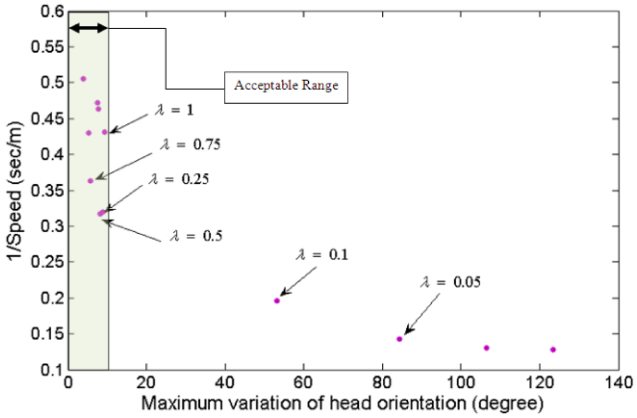

Fig. 10 Maximum variation of head link orientation and robot speed for different values of λ

For the selected value of λ, GA optimization is run with the following settings: Population $N = 20$, Crossover probability $P_c = 0.5$, Mutation probability $P_m = .01$, Number of generations $G = 1000$ and $\theta_{\max} = \pi$. Friction coefficient are also set as $\mu_t = 0.05$ and $\mu_n = 0.56$. Resultant optimized parameters are

$$\alpha = 0.76 \text{ rad}, \qquad \alpha_h = 0.57 \text{ rad}$$
$$\beta = 1.18 \text{ rad}, \qquad \beta_h = -1.46 \text{ rad}$$

The time of simulation is crucial for achieving good results. Stable locomotion is usually reached after short amount of time. Prior to this time, unstable locomotion, we may get a positive fitness score that should be ignored. Therefore, we found, letting the simulation run a certain amount of time before starting the fitness evaluation, solves this problem. In this study, we used the position of the robot after four simulated seconds as starting configuration and its position after thirty seconds as end configuration to measure the displacement of the mass center of the robot.

7.2 Case II

The results obtained in the previous section can be generalized by adding additional parameters that can be optimized. Consider a 5-link snake robot with general sinusoidal form for its relative joint angles.

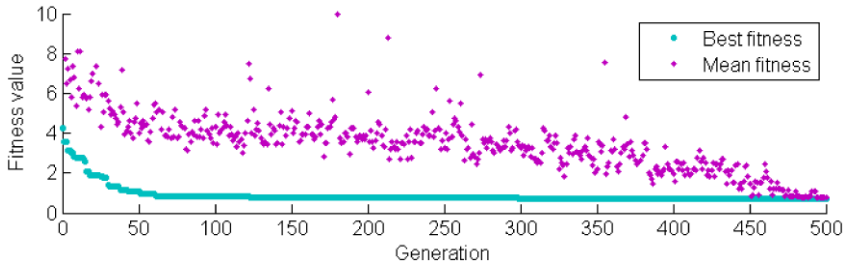

Fig. 11 Development of the best and mean value of fitness for every generation

$$\begin{aligned}\varphi_1 &= \alpha_1 \sin \omega t \\ \varphi_2 &= \alpha_2 \sin(\omega t + \beta_2) \\ \varphi_3 &= \alpha_3 \sin(\omega t + \beta_3) \\ \varphi_h &= \alpha_h \sin(\omega t + \beta_h)\end{aligned} \tag{9}$$

Our objective is to find parameters $\alpha_1, \alpha_2, \alpha_3, \alpha_h, \beta_2, \beta_3$ and β_h which maximize speed while maintaining head link in the direction of motion. In order to do so we use GA with the fitness function defined as in (8). As mentioned in previous section, parameter λ used in fitness function has a considerable effect on results of GA optimization. In order to gain a deeper insight into effects of λ, for this case study (generalized form), we first set λ equal to zero. This lets the robot move with maximum speed without imposing any limitation to the head link orientation. Next, by setting λ equal to 0.25, we force GA to find parameters that result in motion with high speed while orientation of the head also remains in an acceptable range.

7.2.1 Setting $\lambda = 0$

In this case, GA is used to search for optimal FHS gait parameters ($\alpha_1, \alpha_2, \alpha_3, \alpha_h, \beta_2, \beta_3$ and β_h). Equation (8) with setting λ equal to zero is the fitness function that should be minimized. The resultant length of chromosomes becomes 112-bit. Values of $\alpha_1 \sim \alpha_3$ and α_h are bounded to maximum value of $\theta_{\max}$. This parameter represents mechanical limit of motor rotation angle. GA Conditions are set to: Population $N = 20$, Crossover probability $P_c = 0.5$, Mutation probability $P_m = .01$, Number of generations $G = 500$ and $\theta_{\max} = \pi$. Development of fitness value for one of the optimizations (assumed values: $\mu_t = 0.05, \mu_n = 0.56$ and $\omega = 1$ rad/s) performed in this section is shown in Fig. 11.

As shown in this figure, after 500 generations best fitness value converges to 0.081. This value corresponds to maximum speed of 9.7 cm/sec. We repeat the same procedure for different values of friction coefficients. Each optimization consists of 20×500 evaluation of the fitness function which calls for solving dynamic equation (1) for each evaluation. Each optimization takes about 20 seconds. Obtained optimal values are shown in Figs. 12 and 13. Therefore, the optimized values for $\alpha_1, \alpha_2, \alpha_3, \alpha_h, \beta_2, \beta_3$ and β_h depend on friction coefficients and can be selected. Because we used

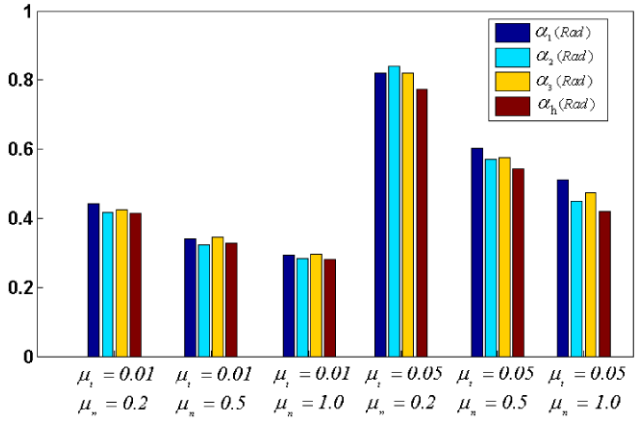

Fig. 12 Optimized $\alpha_1 \sim \alpha_h$ for different friction coefficients ($\lambda = 0$)

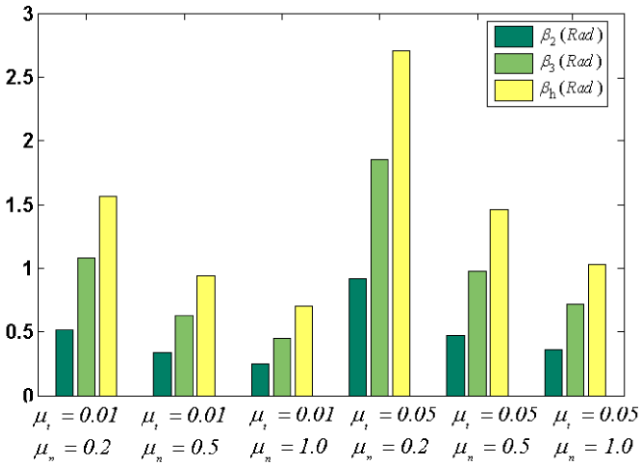

Fig. 13 Optimized $\beta_2 \sim \beta_h$ for different friction coefficients ($\lambda = 0$)

friction coefficients of glass and wood, we can state that the range of friction coefficients used in these optimizations covers a fairly wide range of surfaces. By further inspection of Figs. 12 and 13, the following conclusions may be stated:

- Regardless of friction coefficients values, following equation is true for optimized phase shifts, $\beta_2 \sim \beta_h$

$$\beta_3 = 1.9\beta_2, \qquad \beta_h = 2.9\beta_2 \tag{10}$$

- For any friction coefficients, there are not considerable differences in values of optimized maximum angular deflection, $\alpha_1 \sim \alpha_h$ (Fig. 12).
- Optimum values of $\alpha_1 \sim \alpha_h$ decrease with increasing μ_n and increase with increasing μ_t (Fig. 12).
- Optimum values of phase shift decrease with increasing μ_n and increase with increasing μ_t (Fig. 13).

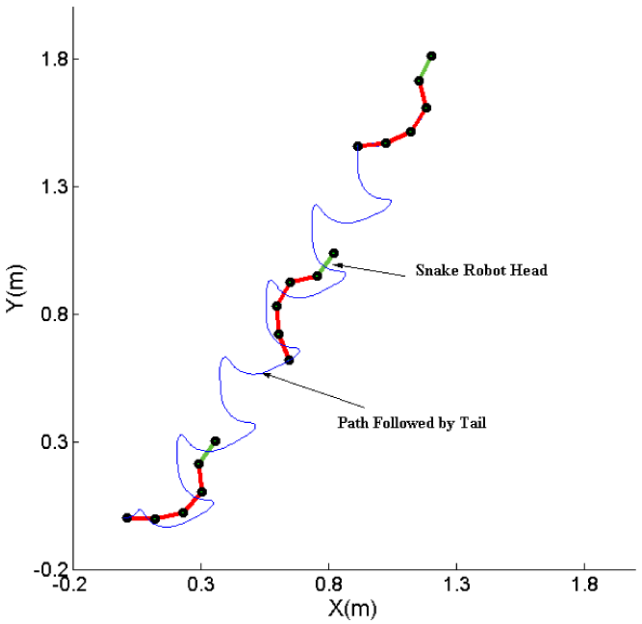

Fig. 14 Snake robot moving with optimized FHS gait ($\mu_t = 0.05$, $\mu_n = 0.56$)

7.2.2 *Setting* $\lambda = 0.25$

Following the procedure of selecting λ discussed in Sect. 7.1, we found letting λ equal to 0.25 for the general case also resulted in appropriate solution. Therefore, (8) with λ equal to 0.25 will be the fitness function that should be minimized. GA settings similar to those of Sect. 7.2.1 are selected. Results indicate that by setting λ equal to 0.25, orientation of the head link remains in an acceptable range of 9.3 degrees while snake robot moves with speed of 7.2 cm/sec. The optimized parameters are

$$\alpha_1 = 1.54 \text{ rad}, \quad \alpha_2 = 1.39 \text{ rad}$$
$$\alpha_3 = 1.44 \text{ rad}, \quad \alpha_h = 1.08 \text{ rad}$$
$$\beta_2 = 0.84 \text{ rad}, \quad \beta_3 = 2.05 \text{ rad}, \quad \beta_h = 4.11 \text{ rad}$$

The resulting motion of robot is shown in Fig. 14. Also note that tail link has significantly more amplitude of undulation than the head link. We repeat the same procedure for different values of friction coefficients. Obtained optimal values are shown in Figs. 15 and 16.

By close inspection of the results illustrated in Figs. 15 and 16, these conclusions can be stated

- There is no clear general relation among optimized values of $\alpha_1, \alpha_2, \alpha_3$ and α_h for specific friction coefficients of the ground. This comes from the fact that by setting λ to a nonzero value, GA tries to make a compromise between higher speed and smaller angular variation of the head. In this situation there are many near optimal solutions that are rather acceptable.
- Regardless of friction coefficients values optimum β_2 is larger than β_3 and β_3 is larger than β_h.

Fig. 15 Optimized $\alpha_1 \sim \alpha_h$ for different friction coefficients ($\lambda = 0.25$)

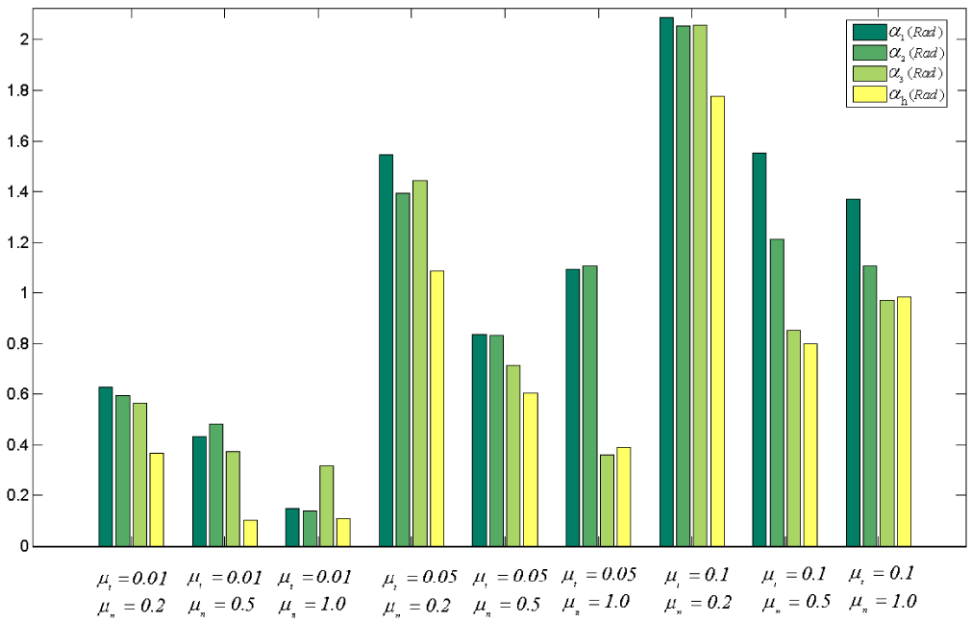

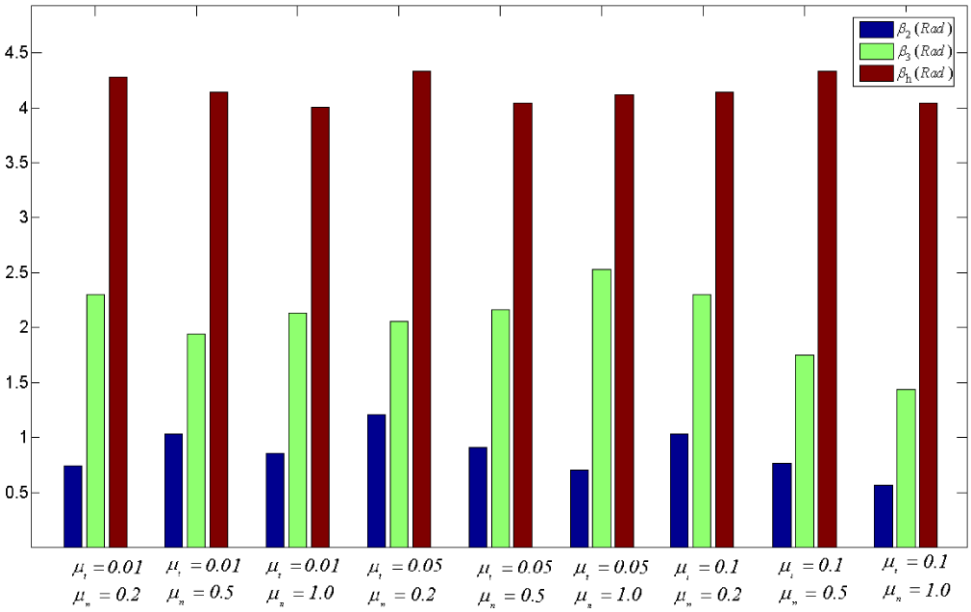

Fig. 16 Optimized $\beta_2 \sim \beta_h$ for different friction coefficients ($\lambda = 0.25$)

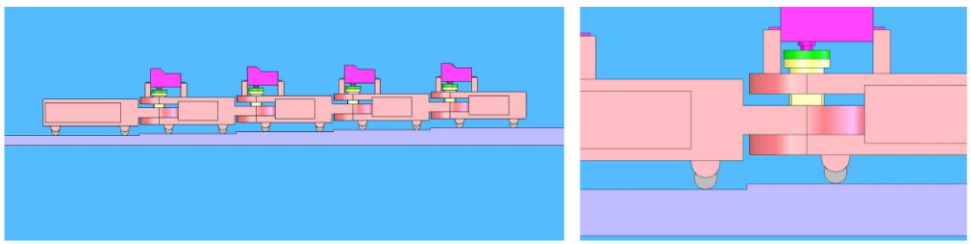

Fig. 17 Schematic view of the physical robot

- Optimum values of $\alpha_1 \sim \alpha_h$ decrease with increasing μ_n and increase with increasing μ_t (Fig. 15).
- There are not considerable differences in values of optimized phase shifts, β_2, β_3 and β_h with different friction coefficients (Fig. 16).

These results can be directly used in a look-up table by robot controller to select optimal values for maximum angular deflection $(\alpha_1, \alpha_2, \alpha_3, \alpha_h)$ and phase shift $(\beta_2, \beta_3, \beta_h)$ in different environmental conditions. An adaptive controller will then be able to insure FHS gait while speed is maximized.

For example, for an environmental condition case ($\mu_t = 0.05$, $\mu_n = 0.56$) the following values are selected:

$$\alpha_1 = 0.83 \text{ rad}, \quad \alpha_2 = 0.83 \text{ rad}$$
$$\alpha_3 = 0.71 \text{ rad}, \quad \alpha_h = 0.60 \text{ rad}$$
$$\beta_2 = 0.91 \text{ rad}, \quad \beta_3 = 2.16 \text{ rad}, \quad \beta_h = 3.48 \text{ rad}$$

8 Experimental results

In order to experimentally evaluate the results obtained in previous sections, an undulatory robotic prototype has been developed, using off-the-shelf components and conventional fabrication techniques. The prototype used in the present study, shown in Fig. 17, is composed of five Plexiglas links (each link: weight 80 g, length 110 mm, width 40 mm and height 30 mm) with the rotary joints actuated by high-torque servo-motors. As illustrated in Fig. 17, special design of the robot joints allows vertical motion of links which makes its motion easier when encountering uneven terrains. Mounted on each joint is a 1.7 W dc motor (Bluebird) with an embedded encoder. The internal timer in the microcontroller insures that all motors are synchronized. Each link of the robot is equipped with four wheels which provide differential friction in the tangential and normal directions of motion. An on-board microcontroller unit (AP Mega16) is used to generate the propulsive wave. The system is powered by on-board batteries or alternatively an external power supply during extended testing sessions.

8.1 Realization of serpentine gait

All simulation results obtained thus far have used the derived dynamic equations. In order to validate dynamic equation of the robot, (1), we adjust geometrical parameters

(length, mass, link inertia) to represent the physical model. The coefficients of tangential and normal frictions for the actual surface are physically measured and are found to be $\mu_t = 0.05$ and $\mu_n = 0.56$. We apply relative angles equation, (4), to both simulation and physical model (with values of $\alpha = \pi/4$, $\beta = \pi/4$) so that the snake robot moves with serpentine gait. Position of center of the mid link is measured by analyzing pictures taken during robot motion. To do this, a digital camera is held fixed overlooking a fixed area. Every two second an image is taken. The images are next analyzed off line and the position of center of the mid link is manually recorded.

We compare path followed by center of the mid link of the physical robot with simulated model (Fig. 18). Differences between these paths are mainly due to inaccurate friction coefficients and incomplete dynamic equations for ignoring effects such as, joint friction, gear box and small differences between links. Additionally, the controller used on the physical model is open loop therefore, there may be missed encoder counts. Another source of discrepancy between the two results may be due to difficulty in recording the actual path followed by the experimental model. Considering limitations discussed above, it can be concluded that using the dynamic equation a good approximation of the actual motion of the robot can be obtained.

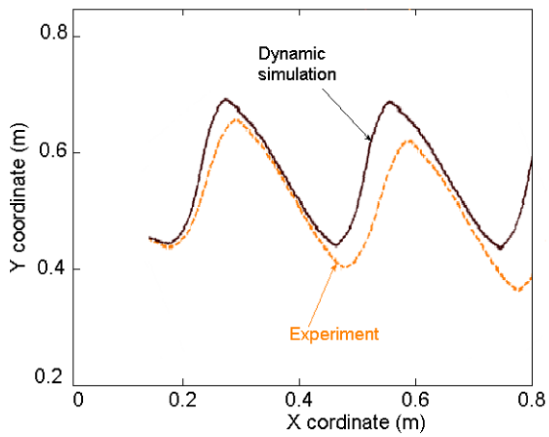

Fig. 18 Comparison of motion predicted by simulation and experimental model

8.2 Realization of FHS gait

To generate FHS gait, we first find FHS parameters by following the procedure explained in Sect. 4. We select $\alpha = \pi/4$, $\beta = \pi/4$ and use GA to obtain FHS parameters $\alpha_h = 0.75$, $\beta_h = -1.98$. The geometrical parameters such as length, mass, moment of inertia, etc of the dynamic model are selected to represent the physical model. Next we drive the motor joints based on (5) and (6). As shown in Fig. 19, numbers 1–4, robot realizes FHS motion and in comparison serpentine motion is realized in numbers 5–8. Clearly the maximum changes in head link angle is significantly lowered, however robot speed is also lowered.

8.3 Realization of adaptive motion using FHS gait

In order to experimentally verify the capability of a ground adaptive controller, we prepared a test bed which allows robot to move on a surface with two different materials, wood and glass. Using one of the robot links, we experimentally calculated friction coefficients of the two surfaces and obtained $\mu_t = 0.05$ and $\mu_n = 0.56$ for glass and $\mu_t = 0.05$ and $\mu_n = 1$ for wood.

Friction coefficients of the ground can be measured online by means of force sensor mounted on the underside wheels (Inoue et al. 2007). In our experiment we calculated these values offline and modified FHS parameters as robot moved from one surface to another. FHS gait parameters for wood and glass surfaces changed when the robot mid-link passed the wood surface. Results shown in Fig. 20 illustrate that by using the proposed adaptive tuner snake robot continues to move with FHS gait on surfaces with different friction coefficients.

8.4 Realization FHS gait with optimized speed

In order to experimentally validate theoretical results obtained in Sect. 7.2.2, we drive motor joints based on the optimized parameters. We measure speed of the robot during certain amount of time. Results are collected in Table 3. Parameters in the first row are optimized parameters obtained in Sect. 7.2.2 which resulted in a relatively higher speed. Parameters of the second and third row are manually selected

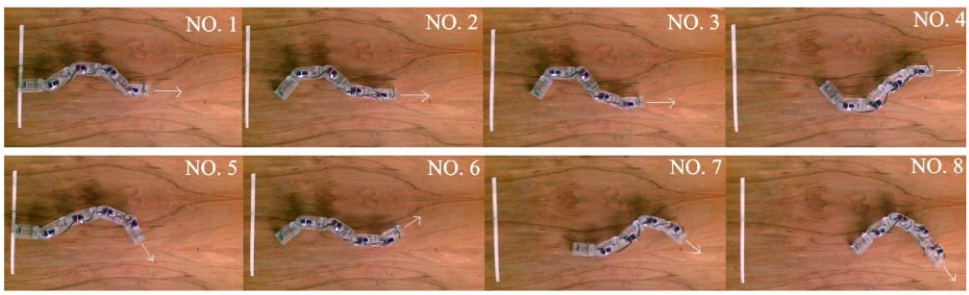

Fig. 19 Comparing FHS and serpentine gaits. 1–4 are FHS gait and 5–8 are serpentine gait

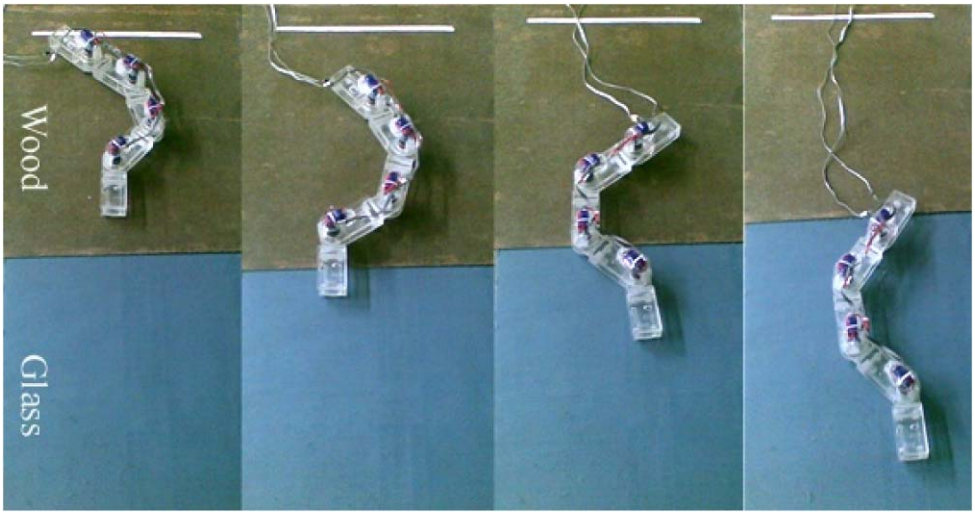

Fig. 20 Snake robot moving on surfaces with different friction coefficients

Table 3 Experimental results

	Parameters (rad)	Measured speed (cm/s)
Optimized case	$\alpha_1 = 0.83, \alpha_2 = 0.83, \alpha_3 = 0.71, \alpha_h = 0.60,$ $\beta_2 = 0.91, \beta_3 = 2.16, \beta_h = 3.48$	1.3
Non optimized case	$\alpha_1 = 0.52, \alpha_2 = 0.52, \alpha_3 = 0.52, \alpha_h = 0.53,$ $\beta_2 = 0.52, \beta_3 = 1.05, \beta_h = -2.31$	0.2
	$\alpha_1 = 1.05, \alpha_2 = 1.05\ \alpha_3 = 1.05, \alpha_h = 1.06,$ $\beta_2 = 0.63, \beta_3 = 1.26, \beta_h = -2.28$	0.7

FHS gait parameters (α_1, α_2, α_3, β_2 and β_3 are randomly selected while α_h and β_h obtained using GA).

9 Conclusion

In this paper, we introduced a novel gait, FHS gait, for a snake robot and compared it with the commonly used serpentine gait. Using the proposed gait, the head link of snake robot remains in the direction of motion. This allows easier sensing of obstacles in environment and therefore greatly enhances the ease of the information processing. We concluded that in spite of similarity and in some cases less efficiency of FHS gait compare to serpentine gait, in terms of power and velocity, FHS gait offers advantages over serpentine gait for applications such as those requiring processing sensory data.

Effects of different friction coefficients on obtained FHS gait were also investigated. Obtained relationships can be used as a base for designing a ground adaptive controller. This controller can ensure FHS motion in different environments.

In order to find FHS gait with maximum speed, we added speed to fitness function of GA. Obtained optimal solution had two characteristics: robot speed was maximized while angular changes of robot head remained in acceptable ranges. We repeated GA multi-objective optimizations for different friction coefficients. Some interesting relationships were obtained between gait parameters and friction coefficients.

In order to validate our theoretical results, we designed and constructed a 5-link snake robot with wheels mounted on each link's underside. Special design of the robot joints allowed vertical motion of links which made its motion easier when encountering uneven trains. We drove robot motor joints using sinusoidal trajectories for which the parameters were obtained by GA. Our experimental robot could realize FHS gait however, small discrepancies exist between path followed by experimental and simulated model.

In order to experimentally verify the capability of a ground adaptive controller, we ran our experimental robot on two surfaces with different friction coefficients. Controller modified gait parameters based on obtained results while robot moved to the new surface. Results indicated maintaining FHS gait on the two surfaces.

This paper is a step toward construction of an autonomous biologically inspired, snake robot with higher intelligence that can be used for applications such as search and rescue. Future research will focus on developing autonomy of the robot by adding obstacle avoidance capability.

References

Burdick, J., Radford, J., & Chirikjian, G. (1995). A 'sidewinding' locomotion gait for hyper-redundant robots. *Advanced Robotics*, *9*(3), 195–216.

Chirikjian, G. S., & Burdick, J. W. (1993). Design and experiments with a 30 DOF robot. In *Proceedings of 1993 IEEE international conference on robotics and automation* (pp. 113–119).

Chirikjian, G., & Burdick, J. (1995). The kinematics of hyper-redundant robot locomotion. *IEEE Transaction on Robotics and Automation*, *11*(6), 781–793.

Choi, H. R., & Ryew, S. M. (2002). Robotic system with active steering capability for internal inspection of urban gas pipelines. *Mechatronics*, *12*(2002), 713–736.

Crespi, A., Badertscher, A., Guignard, A., & Ijspeert, A. J. (2005). Amphibot I: an amphibious snake-like robot. *Robotics and Autonomous Systems*, *50*, 163–175.

Date, H., Hoshi, Y., & Sampei, M. (2000). Locomotion control of a snake-like robot based on dynamic manipulability. In *Proceedings of the 2000 IEEE/RSJ international conference on intelligent robotics and systems* (pp. 2236–2241).

Date, H., Hoshi, Y., Sampei, M., & Nakaura, S. (2001). Locomotion control of a snake-like robot with constraint force attenuation. In *Proceedings of the American control conference* (pp. 113–118).

Dowling, K. (1997). *Limbless locomotion: learning to crawl with a snake robot*. Ph.D. Thesis, Robotics Institute, Carnegie Mellon University, Pittsburgh, PA, December 1997. http://www.societyofrobots.com/robottheory/limbless_locomotion.pdf. Accessed 25 July 2008.

Endo, G., Togawa, K., & Hirose, S. (1999). Study on self-contained and terrain adaptive active cord mechanism. In *Proceedings of the 1999 IEEE/RSJ international conference on intelligent robots and systems* (pp. 1399–1405).

Fukushima, E. F., Hirose, S., & Hayashi, T. (1998). Basic manipulation considerations for the articulated body mobile robot. In *Proceedings of the 1998 IEEE/RSJ international conference on intelligent robots and systems* (pp. 386–393).

Hirose, S. (1993). *Biologically inspired robots (snake-like locomotor and manipulator)*. London: Oxford University Press.

Hirose, S., & Morishima, A. (1990). Design and control of a mobile robot with an articulated body. *The International Journal of Robotics Research*, *9*(2), 99–114.

Ijspeert, A. J. (2001). A connectionist central pattern generator for the aquatic and terrestrial gaits of a simulated salamander. *Biological Cybernetics*, *85*(5), 331–348.

Inoue, K., Sumi, T., & Ma, S. (2007). CPG-based control of a simulated snake-like robot adaptable to changing ground friction. In *Proceedings of IEEE/RSJ international conference on intelligent robots and systems (IROS 2007)* (pp. 1957–1962).

Klaassen, B., & Paap, K. L. (1999). GMD-SNAKE2: a snake-like robot driven by wheels and a method for motion control. In *Proceedings of 1999 IEEE international conference on robotics and automation (ICRA 1999)* (pp. 3014–3019).

Ma, S., Araya, H., & Li, L. (2002). Development of a creeping snaker-obot. *International Journal of Robotics and Automation*, *17*(4), 146–153.

Matsuno, F., & Sato, H. (2005). Trajectory tracking control of snake robots based on dynamic model. In *Proceedings of IEEE international conference on robotics and automation*.

McIsaac, K. A., & Ostrowski, J. P. (2000). A geometric approach to gait generation for the anguilliform robot. In *Proceedings of the international conference on intelligent robots and systems (IROS 2000)* (pp. 2230–2235).

Prautsch, P., & Mita, T. (1999). Control and analysis of the gait of snake robots. In *Proceedings of the 1999 IEEE international conference on control applications* (pp. 502–507).

Prautsch, P., Mita, T., & Iwasaki, T. (2000). Analysis and control of a gait of snake robot. *Transactions of the Institute of Electrical Engineers of Japan*, *120-D*(3), 372–381.

Saito, M., Fukaya, M., & Iwasaki, T. (2002). Serpentine locomotion with robotic snakes. *IEEE Control Systems Magazine*, *22*(2002), 64–81.

Tanev, I., Ray, T., & Buller, A. (2005). Automated evolutionary design, robustness, and adaptation of sidewinding locomotion of a simulated snake-like robot. *IEEE Transactions on Robotics*, *21*(4), 632–645.

Umetani, Y., & Hirose, S. (1976). Biomechanical study of active cord mechanism with tactile sensors. In *Proceedings of the 6th international symposium on industrial robots* (c1-1–c1-10).

Ute, J., & Ono, K. (2002). Fast and efficient locomotion of a snake robot based on self-excitation principle. In *Proceedings of the 7th international workshop on advanced motion control* (pp. 532–539).

Shahir Hasanzadeh received his M.Sc. in Mechanical Engineering in 2008 in Ferdowsi University of Mashhad. He is a candidate of doctoral research at Ferdowsi University of Mashhad, Iran.

Ali Akbarzadeh Tootoonchi received his Ph.D. in Mechanical Engineering in 1997 from University of New Mexico in USA. He worked at Motorola USA for 15 years where he led research and development teams. He joined Ferdowsi University of Mashhad in 2005. His areas of research include, Robotics (Biologically inspired Robots, Parallel Robots, Biped), dynamics, automation and Engineering Statistics.